

# Electron localization in pure and defective ceria by a unified LDA+U approach

Stefano Fabris, Stefano de Gironcoli, and Stefano Baroni  
*SISSA and INFN DEMOCRITOS National Simulation Center,  
Via Beirut 2-4, I-34014 Trieste, Italy*

(Dated: October 24, 2018)

## Abstract

The electronic and structural properties of pure and defective cerium oxide are investigated using a unified LDA+U approach which allows to treat the different valence states of Ce occurring for different stoichiometries on a same ground, without any *a priori* assumptions on the defect chemistry. The method correctly predicts the atomistic and electronic structures of the CeO<sub>2</sub> and Ce<sub>2</sub>O<sub>3</sub> bulk phases, as well as the subtle defect chemistry in reduced materials CeO<sub>2-x</sub>, which controls the oxygen storage functionality of cerium-based oxides. The analysis of the energetics highlights the limits of the LDA+U method and possible extensions are proposed.

Ceria based materials are among the key components of many advanced catalysts used to produce hydrogen and to reduce air pollution. The actual catalyst is a complex device which couples the high chemical activity of noble metals to the thermo-chemical stability of oxide substrates. Besides providing a resistant support for the metal, ceria-based substrates take an active role in the catalytic reaction by controlling the oxygen partial pressure at the reaction sites, acting effectively as oxygen reservoirs. The accepted qualitative mechanism of this phenomenon is based on the following defect chemistry. A reduction of the oxygen partial pressure promotes the release from the crystal lattice of atomic oxygen which, after diffusing to the surface, recombines and desorbs as  $O_2$  gas. The process leaves a charged vacancy in the lattice,  $V_{\text{O}}^{\bullet\bullet}$ , which is neutralized by the valence change  $Ce^{4+} \rightarrow Ce^{3+}$  of two cations (substitutional  $Ce'_{\text{Ce}}$  defects). The release of one oxygen atom from the substrate drives therefore a fundamental change in the electronic structure, leaving two electrons in  $f$ -like empty states. Electronic correlation, due to the strong localization of these states, have the effect of splitting the  $f$  band upon occupation, resulting in a fully occupied gap state at 1.5 eV above the top of the valence band [1, 2, 3]. As a consequence, reduced oxides,  $CeO_{2-x}$ , all result to be insulating. The electron population of this state is directly correlated to the number of  $Ce^{3+}$  ions, and it is employed as an estimator of the concentration of oxygen vacancies [1].

The localization of electrons on atomic-like  $f$  states involves strong correlation effects which are not captured by the most standard implementations of density functional theory (DFT). As a consequence of this, existing first-principles calculations [4, 5, 6, 7] fail to provide a unified picture of the different oxidation states of Ce occurring in ceria. As a matter of facts, all of them adopt either one of the following two assumptions, which are individually appropriate to different oxidation states of Ce, but conflicting with one another: *i*) in the core-state model (CSM) Ce  $f$ -states are treated as part of the core, and therefore their contribution to the bonding process is totally neglected [4]; *ii*) the valence-band model (VBM), instead, treats Ce  $f$  electrons explicitly as valence electrons which are therefore allowed to contribute to the chemical bond [4, 6, 7]. The former approach provides good structural properties for  $Ce_2O_3$  but not for  $CeO_2$  (see Table I), and it describes the oxide as an insulator *by construction*. Most importantly its predictive power is limited: the distribution of  $Ce^{4+}$  or  $Ce^{3+}$  ions has to be assumed as an input of the calculation. As a consequence, the defect chemistry, which we have seen to be determined by the valence change of Ce atoms,

is difficult to access. On the opposite side, the VBM leads to good structural properties for  $\text{CeO}_2$  but not for  $\text{Ce}_2\text{O}_3$  (Table I), and describes this latter structure as a metal. Neither of the two approaches predicts the existence of the gap state experimentally observed to occur in partially reduced ceria  $\text{CeO}_{2-x}$ , therefore failing to describe the localization-delocalization transition of  $f$  states, which is at the basis of the oxygen-storage mechanism.

In the present work these difficulties are overcome using an LDA+U approach which allows to describe all the Ce atoms within a single, unified, approximation regardless of their oxidation state. This is particularly important in the study of complex, heterogeneous, systems—such as *e.g.* a molecule adsorbed on an oxide-supported metal nano-particle—where the oxidation state of each Ce atom is not known in advance. Electron correlations within Ce  $f$  states are modeled by a Hubbard  $U$  contribution added to the traditional density-functional self-consistent potential. The method describes explicitly the  $f$  states and is highly predictive: it correctly describes the electronic structure of pure and defected cerias (always predicted to be insulators); it captures the valence change due to non-stoichiometry (and the related features in the electronic structure); and it allows the intrinsic defects  $\text{Ce}'_{\text{Ce}}$  to occupy the most energetically favorable position with respect to  $\text{V}_{\text{O}}$  without any *a priori* assumptions on their relative geometry. Moreover, it allows to estimate the formation energetics for pure and defective ceria phases, which turn out to be consistent with experiments.

The results presented in this work were obtained by ab initio DFT-based calculations employing the local density approximation for the exchange and correlation potential, and were performed with the PWscf package [8]. The crystal valence wave functions were represented by a plane-waves basis set limited by the kinetic energy of 30 Ry. Their interactions with nuclei and core electrons were described by non-local ultrasoft pseudopotentials [9] constructed for the following atomic configurations: O  $2s^22p^4$ , and Ce  $5s^25p^66s^25d^14f^1$ . The Hubbard  $U$  contribution to the energy functional was treated after the formulation of Cococcioni and de Gironcoli [10, 11]. The on-site parameter  $U$  for Ce was fixed to 3 eV, following the analysis of Ref. 12 where it was estimated with a variational method to lie between 3 and 3.5 eV. Two concentrations of vacancies were considered in the analysis of defective cerias  $\text{CeO}_{2-x}$ :  $x = 0.125$  and  $x = 0.03125$ . The defects were modeled with the supercell method by removing one oxygen atom from the supercells containing, respectively, 24 and 96 atomic sites.

The LDA+U energy functional reads:

$$E_{LDA+U} = E_{LDA} + \frac{U}{2} \sum_I \text{Tr} (\mathbf{n}^I (\mathbf{1} - \mathbf{n}^I)), \quad (1)$$

where the  $\mathbf{n}^I$ 's are  $M \times M$  matrices ( $M$  being the degeneracy of the localized atomic orbital,  $M = 14$  in the case of  $f$  orbitals), projections of the one-electron density matrix,  $\hat{\rho}$ , over the  $f$  manifold localized at lattice site  $I$ :

$$\langle \phi_{m\sigma}^I | \hat{\rho} | \phi_{m'\sigma'}^I \rangle = n_{mm'}^{I\sigma} \delta_{\sigma\sigma'}. \quad (2)$$

In the above equation  $\phi_{m\sigma}$  denotes a localized (spin) orbital, with angular and spin quantum numbers  $m$  and  $\sigma$ , and the orthonormality over the spin variables is a consequence of the collinearity of the spin structure. The second term in Eq. (1), which we call  $E_U$ , is positive definite for  $U > 0$  because the eigenvalues of the  $\mathbf{n}^I$  matrices—*i.e.* the occupation numbers of the  $f$  orbitals—lay in the range  $[0, 1]$ . Note that, as soon as  $U$  is large enough to open a gap between occupied and unoccupied  $f$  states, the effect of  $E_U$  is to favor the  $f$  occupation numbers to be close to either 0 or 1. At these extremes,  $E_U$  is strictly 0 and the total energy is back to the LDA value.

Ceria is known to exist in the cubic fluorite-type  $\text{CeO}_2$  ( $Fm\bar{3}m$ ) and the hexagonal  $A$ -type  $\text{Ce}_2\text{O}_3$  ( $P\bar{3}m1$ ) bulk phases. The latter can be considered as a highly defective  $\text{CeO}_2$  structure where one every four oxygen atoms is missing, with the vacancies being ordered along non intersecting  $\langle 111 \rangle$  directions, and with all the Ce ions nominally in the 3+ valence state [5]. The  $\text{Ce}_2\text{O}_3$  structure is anti-ferromagnetic [13], therefore the calculations for this phase were carried out in the local-spin-density approximation.

The calculated structural properties for the bulk polymorphs are summarized in Table I and are in good agreement with experiments. The Hubbard contribution to the energy functional increases the lattice parameter by 0.4% in  $\text{CeO}_2$  and by 2.5% in  $\text{Ce}_2\text{O}_3$  with respect to the LDA values. Note how the LDA+U approach provides a good prediction of the structural properties for both polymorphs, therefore combining the achievements of the VBM for  $\text{CeO}_2$  with the ones of the CSM for  $\text{Ce}_2\text{O}_3$ .

The density of electronic states (DOS) for the two polymorphs calculated at the equilibrium lattice parameters are shown in Figure 1. Occupied states are indicated by shaded areas, and the zero energy is the top of the upper valence band (with prevalent O-2p character). For  $\text{CeO}_2$  (Figure 1a), the sharp band centered at  $\approx 3$  eV is formed by fairly

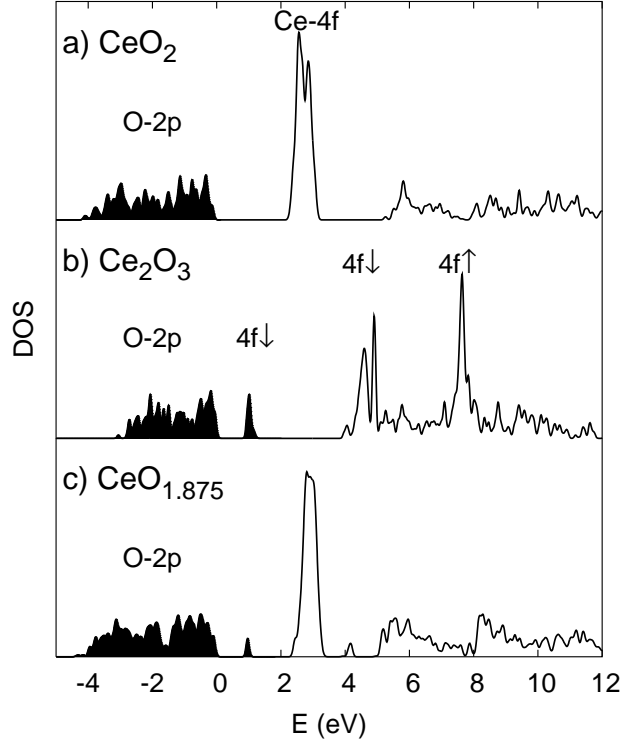
TABLE I: Calculated structural properties of the bulk  $\text{CeO}_2$  and  $\text{Ce}_2\text{O}_3$  phases compared with previous theoretical values in the valence-band and core-state models (VBM and CSM), and with experimental measurements.

	$\text{CeO}_2$		$\text{Ce}_2\text{O}_3$		
	$a_0$ [ $\text{\AA}$ ]	$B$ [GPa]	$a_0$ [ $\text{\AA}$ ]	$c/a$	$B$ [GPa]
LDA VBM Ref. 5	5.39	214.7	3.72	1.55	208.6
LDA CSM Ref. 5	5.56	144.9	3.89	1.55	165.8
LDA+U This work	5.41	210.6	3.81	1.55	149.8
Expt.	5.41	204-236	3.88	1.55	–

localized atomic-like Ce-4*f* empty orbitals. The onset of the conduction band is 5.1 eV above the highest occupied state, exhibiting the typical LDA underestimate with respect to the measured gap of 6.0 eV [14] (following Ref. [14] we do not consider the *f*-manifold as conduction states). The calculated electronic structure for  $\text{Ce}_2\text{O}_3$  is in good agreement with experiments: it predicts an anti-ferromagnetic insulator, with a magnetic moment of  $2.25 \mu_{\text{B}}/\text{molec}$  (the experimental value is  $2.17 \mu_{\text{B}}/\text{molec}$  [13]). The corresponding DOS is displayed in Figure 1b, showing a splitting between occupied and unoccupied states within the *f* manifold. Due to the effects of the Hubbard energy term, the Ce-4*f* states do not form one single band — as in the  $\text{CeO}_2$  structure or in previous VBM calculations — but are split in three energy regions: a doubly occupied state at  $\approx 1.2$  eV above the top of the valence O-2*p* band and corresponding to electrons localized on the  $\text{Ce}^{3+}$  atoms (with alternating spins along the *z* axis). The position and intensity of this peak (relative to the O-2*p* band) are in excellent agreement with experimental photoemission measurements [2]. In the range of *U* suggested by Ref. [12] (3-3.5 eV), the energy of the gap state depends linearly on *U* spanning the values between 1.2 and 0.9 eV (with respect to the top of the valence band). The remaining 13 *f* states are also split in two bands centered at 4.5 and 7.5 eV, and grouping the 6 and 7 states having their spin parallel and anti-parallel to the one of the electron localized on their respective site.

An oxygen vacancy is formed by removing a neutral oxygen atom from a  $\text{CeO}_2$  supercell. As a consequence, two electrons have to be accommodated in the *f* states above the Fermi

FIG. 1: Density of electronic states for pure  $\text{CeO}_2$  (a) and  $\text{Ce}_2\text{O}_3$  (b) bulk phases, and for defective (c) ceria structures  $\text{CeO}_{2-x}$ . Occupied states are indicated as shaded areas, and the zero energy is set to the top of the valence band.



energy of Figure 1a. Our LDA+U model predicts the localization of two electrons on two Ce atoms neighboring the vacancy. This has the effect of formally modifying the valency of Ce from +4 to +3. This result is in agreement with the experimental evidence that the compensating defects are  $\text{Ce}'_{\text{Ce}}$  which tend to cluster around the oxygen vacancy, forming a defect aggregate. An electronic configuration in which two electrons were initially localized on Ce atoms far from the vacancy led to the same self-consistent solution with the Ce nearest neighbors to the vacancy being formally  $\text{Ce}^{3+}$ . Upon removal of an oxygen atom, the O atoms neighbouring the vacancy relax toward the vacancy by  $\approx 0.125 \text{ \AA}$ , and the Ce atoms outward by  $\approx 0.08 \text{ \AA}$ . Moreover, the O atoms neighbouring the  $\text{Ce}'_{\text{Ce}}$  relax away from these defects (see our previous description on the supercells used to model these systems). The DOS for a model of defective ceria,  $\text{CeO}_{2-x}$ , is shown in Figure 1c for  $x = 0.125$ . One sees that the DOS displays in this case features which are intermediate between those of the  $\text{Ce}_2\text{O}_3$  and  $\text{CeO}_2$  structures: the gap state at  $\approx 1.2 \text{ eV}$  (due to occupied  $f$  states on  $\text{Ce}^{3+}$  atoms as in  $\text{Ce}_2\text{O}_3$ ), and the sharp unoccupied  $f$  band of the  $\text{Ce}^{4+}$  atoms at 3

eV. The position and relative weight of the peak corresponding to the occupied gap state are in excellent agreement with observed photoemission spectra [1, 2, 3]. In Figure 2a we display the integrated charge density corresponding to the gap state in  $\text{CeO}_{2-x}$ . This figure demonstrates that, in these dilute regimes, the effects of the formation of a vacancy on the electronic structure are limited to the first shell of atoms around the defects (vacancy and compensating  $\text{Ce}^{3+}$ ).

Let us now examine the energetics of reduction of ceria, and focus in particular on the two reactions: the  $\text{CeO}_2$ - $\text{Ce}_2\text{O}_3$  transition,  $2\text{CeO}_2 \rightarrow \text{Ce}_2\text{O}_3 + 1/2\text{O}_2(\text{g})$  (whose enthalpy measured at 298 K is  $-0.58$  Ry [15]), and the formation of a vacancy (whose experimental heat of reduction is  $0.34-0.37$  Ry [16, 17]). The LDA+U approach severely underestimate the energetics of these reactions:  $-0.33$  Ry for the  $\text{Ce}_2\text{O}_3$ - $\text{CeO}_2$  transition, and  $0.26$  Ry for the vacancy formation. This error is not due to the local density approximation itself, since gradient corrected calculations (including the Hubbard term) also led to quite similar underestimates.

The source of this error can be traced back to some details of the implementation of the LDA+U method which are best evidenced by analyzing the occupation matrices, Eq. (2). The integrated charge of the gap state is exactly 2 (one electron for each  $\text{Ce}^{3+}$  atom). Inspection of the isosurface charge density displayed in Figures 2 shows that the the gap state is not localized exclusively on  $\text{Ce}^{+3}$  atoms but has small projections also on the first neighbouring O sites. As a consequence, when this state is projected onto Ce- $f$  orbitals, Eq. (2), the resulting occupation number is clearly smaller than 1 (in fact,  $\approx 0.98$ ). The problem is even more clear in  $\text{CeO}_2$ , where, due to the prevalent ionic bonding, the Ce- $4f$  states should be empty and the occupancies very close to 0. This is not the case, since most of the calculated occupancies are small, but not vanishing (in fact,  $\approx 0.01-0.02$ ). In the particular case of the  $xyz$  component, which points along the Ce-O bond, the occupancy is much larger ( $\approx 0.2$ ). This large value comes from the partial covalent character of the Ce-O bond, has nothing to do with correlation, and should not contribute to the Hubbard energy,  $E_U$ .

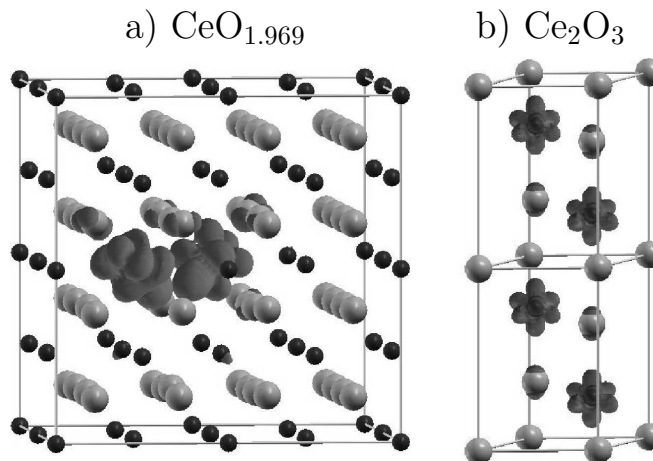
We conclude that the errors in the vacancy formation energy has to be traced back to the spurious occupancies resulting from the particular choice of the projector in (2), which picks up bonding charge from neighbouring O atoms. Nevertheless, in this relatively simple case (where the occupied  $f$  state is well separated from the valence band) a simple and

effective remedy can be found. If the states used to calculate the occupation matrices, Eq. (2), instead of being the atomic Ce- $f$  states, were those resulting *self-consistently* from the calculation (*i.e.* the Wannier functions of prevalent Ce- $f$  character), then the occupancy corresponding to the gap state would be one, and that corresponding to other orbitals of prevalent Ce- $f$  character zero, *by construction*. This argument shows that—in the present situation where the split state is well separated from all the others—a better characterization of the localized orbitals which define  $E_U$  would simply result in a vanishing contribution of  $E_U$  to the final, self-consistent, energy. A quick-and-dirt fixup to the vacancy formation energy problem seems therefore to be to use  $E_U$  to generate the correct electronic structure, but to ignore it altogether in the calculation of the total energy. This amounts to use the LDA+U model to generate the molecular orbitals, and revert to the LDA functional for the calculation of energies. With this extremely simple scheme, also the energetics of the two reactions result in good agreement with experiments:  $-0.610$  Ry for the  $\text{Ce}_2\text{O}_3\text{-CeO}_2$  transition (experimental value is  $-0.58$ Ry [15]), and  $0.361$  Ry for the vacancy formation (experimental values are  $0.34\text{--}0.37$  Ry [16, 17]).

We stress that the dependence of the results on the projector used to define the occupancies is important on the energetics, but have little effect on the electronic structure. The atomistic and electronic structures of pure and defective cerias, as well as their energetics, can therefore be captured by a *modified* LDA+U method which takes advantage of the Hubbard  $U$  effect (essential for giving the correct description of the electrons) in the self-consistent electronic problem, and whose energy has been “corrected” a posteriori to account for the spurious occupancies due to partially covalent character of the chemical bond.

In summary, the LDA+U method provides a simple and accurate way to account for the subtle mechanism of  $f$ -electron localization-delocalization which determines the mixed valence character of Ce and which is at the basis of the oxygen storage properties of ceria. This method is accurate and predictive, opening the way to the *ab-initio* study of complex structures of technological interest—such as *e.g.* ceria-supported metal nanoparticles—which cannot be easily treated by more empirical approaches where the valence state of individual Ce atoms is pre-assigned. Limitations of this approach show in the calculation of reduction/oxidation energies, which can however be fixed in the present case by a simple prescription on the energy functional.

FIG. 2: Isosurface in the charge density (grey) corresponding to the occupied gap-state in  $\text{CeO}_{1.969}$  (left) and  $\text{Ce}_2\text{O}_3$  (right). Black and light grey circles denote Ce and O atoms.



We wish to thank J. Kaspar for prompting our interest in this subject and for fruitful discussions. We are also grateful to G. Balducci for many fruitful discussions and for allowing us to use data from Ref. 12 prior to publication. Calculations have been made possible by the SISSA-CINECA scientific agreement and by the allocation of computer resources from INFN Progetto Calcolo Parallelo Computer. Molecular graphics has been generated with the XCrySDen software [18].

- 
- [1] M. A. Henderson, C. L. Perkins, M. H. Engelhard, S. Thevuthasan, and C. H. F. Peden, *Surf. Sci.* **526**, 1 (2003).
  - [2] D. R. Mullins, P. V. Radulovic, and S. H. Overbury, *Surf. Sci.* **429**, 186 (1999).
  - [3] A. Pfau and K. D. Schierbaum, *Surf. Sci.* **321**, 71 (1994).
  - [4] N. V. Skorodumova, R. Ahuja, S. I. Simak, I. A. Abrikosov, B. Johansson, and B. I. Lundqvist, *Phys. Rev. B* **64**, 115108 (2001).
  - [5] N. V. Skorodumova, S. I. Simak, B. I. Lundqvist, I. A. Abrikosov, and B. Johansson, *Phys. Rev. Lett.* (2002).
  - [6] S. Gennard, F. Corà, and C. R. A. Catlow, *J. Phys. Chem. B* **103**, 10158 (1999).
  - [7] J. C. Conesa, *J. Phys. Chem. B* **107**, 8840 (2003).
  - [8] S. Baroni, A. D. Corso, S. de Gironcoli, and P. Giannozzi, <http://www.pwscf.org>.
  - [9] D. Vanderbilt, *Phys. Rev. B* **41**, 7892 (1990).

- [10] M. Cococcioni, Ph.D. thesis, International School for Advanced Studies (SISSA) (2002), available at <http://www.sissa.it/cm/phd.php>.
- [11] M. Cococcioni and S. de Gironcoli, unpublished.
- [12] G. Balducci and S. de Gironcoli, unpublished.
- [13] H. Pinto, M. N. Mintz, M. Melamud, and H. Shaked, *Phys. Lett. A* **88**, 81 (1982).
- [14] E. Wuilloud, B. Delley, W. D. Schneider, and Y. Baer, *Phys. Rev. Lett.* **53**, 202 (1984).
- [15] D. R. Lide, ed., *CRC Handbook of Chemistry and Physics* (CRC press, Inc, 1993).
- [16] H. L. Tuller and A. S. Nowick, *J. Electrochem. Soc.* **122**, 255 (1975).
- [17] E. K. Chang and R. N. Blumenthal, *J. Solid State Chem.* **72**, 330 (1988).
- [18] A. Kokalj, *J. Mol. Graphics Modelling* **17**, 176 (1999).